Biochimica et Biophysica Acta 1784 (2008) 1728-1734

Contents lists available at ScienceDirect

Biochimica et Biophysica Acta

journal homepage: www.elsevier.com/locate/bbapap

Thermal unfolding of *Escherichia coli* trigger factor studied by ultra-sensitive differential scanning calorimetry

Dong-Jie Fan [a,c], Yan-Wei Ding [b], Xian-Ming Pan [a], Jun-Mei Zhou [a,*]

[a] National Laboratory of Biomacromolecules, Institute of Biophysics, Chinese Academy of Sciences, 15 Datun Road, Chaoyang District, Beijing 100101, China
[b] Hefei National Laboratory for Physical Science at Microscale, University of Science and Technology of China, Hefei 230026, China
[c] Graduate School of the Chinese Academy of Sciences, 19 Yuquan Road, Shijinshan District, Beijing 100039, China

ARTICLE INFO

Article history:
Received 21 March 2008
Received in revised form 22 April 2008
Accepted 8 May 2008
Available online 18 May 2008

Keywords:
Cross-linking
DSC
Intermediate
Protein folding
Thermal denaturation
Trigger factor

ABSTRACT

Temperature-induced unfolding of *Escherichia coli* trigger factor (TF) and its domain truncation mutants, NM and MC, were studied by ultra-sensitive differential scanning calorimetry (UC-DSC). Detailed thermodynamic analysis showed that thermal induced unfolding of TF and MC involves population of dimeric intermediates. In contrast, the thermal unfolding of the NM mutant involves population of only monomeric states. Covalent cross-linking experiments confirmed the presence of dimeric intermediates during thermal unfolding of TF and MC. These data not only suggest that the dimeric form of TF is extremely resistant to thermal unfolding, but also provide further evidence that the C-terminal domain of TF plays a vital role in forming and stabilizing the dimeric structure of the TF molecule. Since TF is the first molecular chaperone that nascent polypeptides encounter in eubacteria, the stable dimeric intermediates of TF populated during thermal denaturation might be important in responding to stress damage to the cell, such as heat shock.

1. Introduction

Escherichia coli trigger factor (TF) is an important molecular chaperone in nascent peptide folding [1–4]. TF binds at the ribosome exit tunnel through the interaction of the highly flexible loop in its N-terminal domain with the L23 and L29 proteins of the 50S ribosome subunit [5,6]. Thus TF is the first molecular chaperone that nascent polypeptides encounter [1,2]. Limited proteolysis indicates that TF contains three distinct domains from N-terminal to C-terminal, defined as the N domain (1–145), M domain (146–251) and C domain (252–432) [7,8]. The N-terminal domain of *E. coli* TF is important for ribosome binding [9] and the M domain carries the PPIase activity [1,7]. Crystal structures show that TF forms a protective shield for nascent polypeptides at the ribosome exit tunnel and assists the folding of most newly synthesized polypeptide chains [9–11]. It has been concluded that both the C-terminal domain and part of the N-terminal domain of TF are essential for its chaperone activity [12–14] and the C domain, together with a segment of the N domain, forms the 'back' and 'arms' of the TF structure, which orients its hydrophobic inner surface toward emerging nascent polypeptides [15]. The multi-domain structure of TF makes it an interesting and challenging candidate for folding studies.

Determining the mechanism of protein folding requires structural characterization of the native and unfolded states as well as any partially folded states formed during folding. Multi-domain and multi-subunit proteins are generally observed to fold by stepwise or parallel folding pathways, via one or more partially folded intermediates [16]. In some cases, such intermediates are stable under the conditions of equilibrium experiments, which facilitates study of their structural properties [17–19]. Urea denaturation of TF and its fragments suggests that the three structural domains of TF may fold relatively independently, although no partially folded intermediates have been characterized [8]. In our previous investigation, two distinct intermediates (a native like state and a compact denatured state) were identified and characterized during guanidine denaturation [20]. We suggested that the ability of TF to undergo structural rearrangement, during guanidine denaturation, to maintain enzyme activity while reducing chaperone and dimerization abilities may be related to the physiological function of TF [21]. However, by perturbing the structure of a protein by chemical denaturants, such as urea or guanidine, the intermediates identified may not actually be present under physiological conditions. Calorimetric data can provide a complete thermodynamic characterization as well as a direct experimental evaluation of the folding/unfolding partition function and the population of intermediate states. This approach has been used in numerous calorimetric applications [22] but has not been used in studying the folding/unfolding of trigger factor. To avoid the possibly artificial effects induced by chemical denaturants, we investigated thermal denaturation of TF and its domain truncation mutants, NM and MC, by

* Corresponding author. Tel.: +86 10 6488-9859; fax: +86 10 6484 0672.
E-mail address: zhoujm@sun5.ibp.ac.cn (J.-M. Zhou).

1570-9639/$ – see front matter © 2008 Elsevier B.V. All rights reserved.
doi:10.1016/j.bbapap.2008.05.002

differential scanning calorimetry (DSC). The results show that the thermal unfolding of TF is quite different from that induced by urea or guanidine denaturation. The dimeric state of TF is extremely stable during thermal unfolding leading to population of three dimeric intermediates. By comparing the thermal unfolding of the intact TF molecule and the domain truncation mutants, NM and MC, we provide further evidence that the C-terminal domain of TF plays a vital role in forming and stabilizing the dimeric structure of the TF molecule [23,24].

2. Materials and methods

2.1. Material

Chelating Sepharose fast flow resin was from Amersham Pharmacia. IPTG was purchased from Takara. Disuccinimidyl suberate (DSS) was from Pierce. The plasmid pQE60 containing the wild-type *tig* gene that encodes *E. coli* TF was donated by Professor G. Fisher. Plasmid mini-pRSETa was donated by Dr. M. Bycroft. BamHI, HindIII and T4 DNA ligase were purchased from Promega. All other chemicals were local products of analytical grade.

2.2. Construction, expression and purification of TF and its mutants

The *E. coli* TF genes and its fragments were amplified from vector pQE60 using PCR. The primers corresponding to TF, and NM and MC fragments from 5′ to 3′ were 5′-atcgcggatccatgcaagtttcagttgaaaccactc-3′, 5′-actgaagcttttacgcctgctggttcatc-3′; 5′-atcgcggatccatgcaagtttcagttgaaaccactc-3′, 5′-atcgcaagcttttattctgcagttccggca-3′; 5′-atcgcggatcccagcaggcgacctggaa-3′, 5′-atcgcaagcttttacgcctgctggttcatc-3′ respectively. PCR products were purified by preparative electrophoresis, digested with BamHI and HindIII, then ligated into the vector pRSETa using T4 DNA ligase. The DNA sequence integrity of TF and its mutants NM and MC was confirmed by sequencing. The resulting plasmids for TF (1–432 aa), NM (1–251 aa) and MC (146–432 aa) were transformed into *E. coli* MC4100 and the recombinant proteins with an N-terminal hexa-His-tag were expressed. Cells were grown in 2YT medium and expression was induced with 250 μM final concentration of IPTG (isopropyl-β-D-thiogalactoside). TF and its mutants were eluted from a Ni chelating Sepharose fast flow column. Protein concentrations were determined using calculated extinction coefficients at 280 nm of 15,930 M^{-1} cm^{-1} for TF, 13,846 M^{-1} cm^{-1} for NM and 9978 M^{-1} cm^{-1} for MC, according to the method of Gill and von Hippel [25].

2.3. Calorimetric studies

UC-DSC experiments were performed using a VP-DSC differential scanning microcalorimeter (Hefei National Laboratory for Physical Science of Microscale, China). The protein samples were exhaustively dialyzed before use against 10 mM sodium phosphate buffer, pH 7.8, and the final dialysate was used as a reference solution. Each protein solution and the reference solution were degassed at 15 °C for 15 min and then equilibrated at 15 °C for 30 min before heating. The protein at 1 mg/ml was heated at a rate of 1 °C/min from 15 °C to 90 °C and a constant pressure of 2.2 atm. The reversibility of the thermal transition of TF and its mutants was tested by checking the second calorimetric trace immediately after cooling from the first run. Under our experimental conditions, no aggregation occurred in the heated sample and the second heat capacity peak approximately matched the first heat capacity peak. Deconvolution analysis and plotting of the calorimetric data was performed using Origin software (Microcal Inc.).

2.4. Cross-linking and electrophoresis

TF and its mutants were cross-linked at a concentration of 20 μM with 6 mM DSS in 10 mM sodium phosphate buffer pH 7.8 at different temperatures. After 30 min, the cross-linking reaction was quenched using the same volume of 150 mM Tris–HCl buffer pH 6.8. The products of the cross-linking reaction were analyzed by SDS-PAGE and visualized by Coomassie Brilliant Blue staining.

3. Results and discussion

3.1. Thermal stability of TF and its domain truncation mutants, NM and MC

Thermal unfolding of wild-type TF and its terminal domain truncated mutants, NM and MC, were studied by UC-DSC and the temperature dependence of the excess heat capacity (C_p^{exc}) is shown in Fig. 1. The temperature dependence of the excess heat capacity does not give single symmetrical peaks for any of the three species, suggesting that the thermal unfolding of TF and its mutants are not a simple two state processes. For wild-type TF, the apparent Tm value obtained from the main peak of the thermogram was about 54 °C and two shoulder peaks were observed at lower and higher temperatures

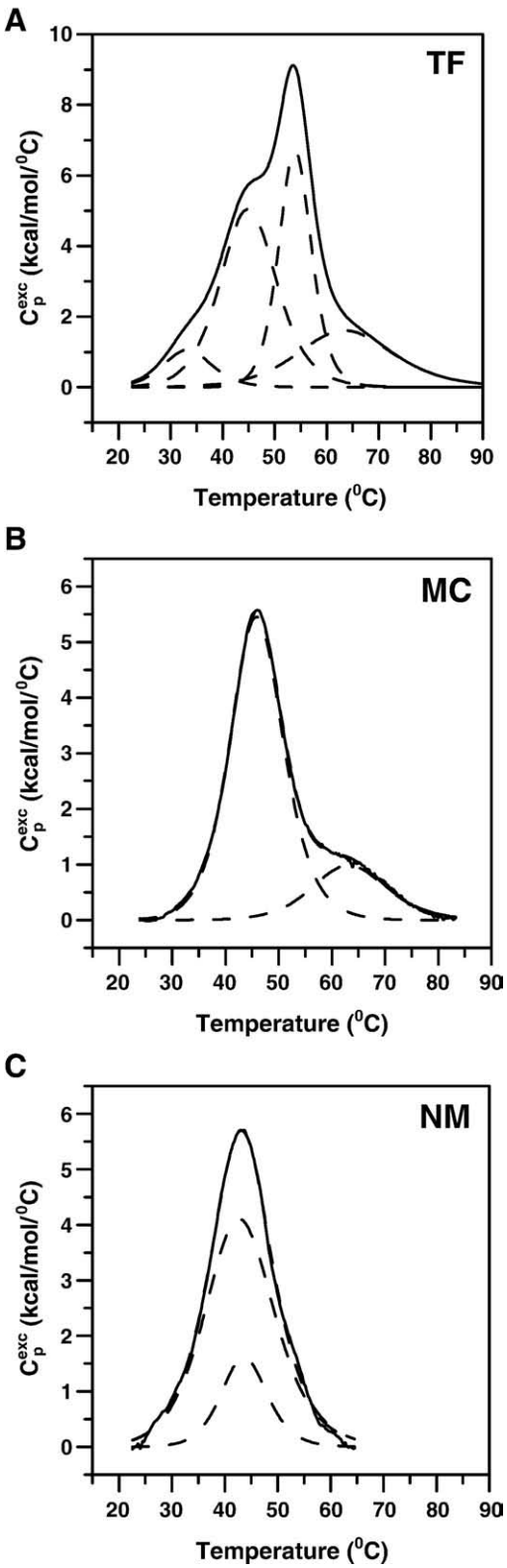

Fig. 1. Normalized and baseline-subtracted thermogram of TF (A), MC (B) and NM (C). The deconvolution curves were given as dashed line. The protein concentration was 1 mg/ml. Buffer conditions were 10 mM sodium phosphate, pH 7.8. The heating rate was 1 °C/min.

(Fig. 1A), suggesting the existence of more than two underlying melting processes. The main peaks of the heat capacity for MC and NM were located at 46 °C and 43 °C respectively (Fig. 1B and C). Clearly, the apparent melting temperatures of NM and MC are significantly reduced by deletion of either the C or the N domain of the TF

molecule. The 11 °C or 8 °C decrease in apparent Tm caused by deletion of the C or N domain indicates a pronounced stabilization of the native structure of the TF molecule by inter-domain interactions.

The complex profile of the curves in Fig. 1 indicates that the thermal unfolding of TF and its terminal truncation mutants proceeds in several overlapping stages over a range of temperatures. The overall endothermic absorption curve appears complex and in order to analyze the absolute heat capacity function we needed to deconvolute the curve on the basis of several simple, two state components of the observed complex process of heat absorption. The individual deconvolution patterns of TF and its mutants are also shown in Fig. 1 (dashed lines). The deconvolution analysis shows that the thermal transition peaks for each protein differ by the peak position, by the amplitudes and by the number of deconvoluted peaks. In order to better understand the detailed process of thermal unfolding of TF and the two domain truncation mutants, we considered a general unfolding reaction in which an initial native state, N, undergoes a conformational transition to the final unfolded state, U, via a series of intermediates states, I_i, to simulate the excess heat capacity (C_p^{exc}) as a function of temperature. The best fit of the data shows that the mechanism of thermal unfolding for TF and the terminal domain truncation mutants, MC and NM, are significantly different. The details are described below.

3.2. Thermal unfolding of TF involves population of three dimeric intermediates

As known from the published crystal structures, TF adopts an unusual extended fold resembling a "crouching dragon" with the N-terminal forming the "tail", the M domain forming the "head", and the C-terminal forming the "arm" and "back" [15,26]. The asymmetric unit of the crystal contains two monomers related by a noncrystallographic twofold symmetry axis and domains I (termed the N domain in this article) and III (the C domain in this article) mediate the dimer formation of TF by wrapping around each other [26]. These interactions lead to the existence of TF in a monomer-dimer equilibrium [27–29] in solution and only native TF forms a dimer in solution during guanidine denaturation [20].

In order to analyze the thermal unfolding of TF, we first assumed a general mechanism for dimeric protein unfolding, $N_2 \overset{K1}{\leftrightarrow} 2N \overset{K2}{\leftrightarrow} 2U$, in which the dimer dissociates to monomer before it unfolds. However, when the data were fitted according to this mechanism, the result was far from satisfactory (not shown). We then tried a number of possible mechanisms for TF thermal unfolding and, finally, the best fit of the data was obtained when assuming that TF is initially dimeric and undergoes thermal unfolding via three dimeric intermediates to the denatured monomeric state, as described below:

$$N_2 \overset{K_1}{\leftrightarrow} I_2^1 \overset{K_2}{\leftrightarrow} I_2^2 \overset{K_3}{\leftrightarrow} I_2^3 \overset{K_D}{\leftrightarrow} 2U$$

At equilibrium,

$$K_1 = \frac{[I_2^1]}{[N_2]} \tag{1}$$

$$K_2 = \frac{[I_2^2]}{[I_2^1]} \tag{2}$$

$$K_3 = \frac{[I_2^3]}{[I_2^2]} \tag{3}$$

$$K_D = \frac{[U]^2}{[I_2^3]} \tag{4}$$

Where K_1, K_2, K_3 and K_D are the equilibrium constants of the individual unfolding processes. Conservation of mass requires that

$$C_0 = [N_2] + [I_2^1] + [I_2^2] + [I_2^3] + [U]/2 \tag{5}$$

Where C_0 is the total concentration of the species present at any temperature. Combining Eqs. (1)–(5), C_0 can be expressed as

$$C_0 = \left(\frac{1}{K_D K_3 K_2 K_1} + \frac{1}{K_D K_3 K_2} + \frac{1}{K_D K_3} + \frac{1}{K_D}\right)[U] + \frac{[U]}{2} \tag{6}$$

Let

$$A = \left(\frac{1}{K_D K_3 K_2 K_1} + \frac{1}{K_D K_3 K_2} + \frac{1}{K_D K_3} + \frac{1}{K_D}\right)$$

$$B = \frac{1}{K_3 K_2 K_1} + \frac{1}{K_3 K_2} + \frac{1}{K_3} + 1$$

$$D = \frac{1}{K_2 K_1} + \frac{1}{K_2} + 1$$

$$E = \frac{1}{K_1} + 1$$

Thus, the concentrations of the states distributed at equilibrium are:

$$[U] = -1/4A + 1/2A\sqrt{4AC_0 + 1/4} \tag{7}$$

$$[I_2^3] = \frac{C_0 - [U]/2}{B} \tag{8}$$

$$[I_2^2] = \frac{C_0 - [U]/2 - [I_2^3]}{D} \tag{9}$$

$$[I_2^1] = \frac{C_0 - [U]/2 - [I_2^3] - [I_2^2]}{E} \tag{10}$$

$$[N_2] = \frac{[I_2^1]}{K_1} \tag{11}$$

and

$$f_U = 2\frac{[U]}{C_0}$$

$$f_{I_2^3} = \frac{[I_2^3]}{C_0}$$

$$f_{I_2^2} = \frac{[I_2^2]}{C_0}$$

$$f_{I_2^1} = \frac{[I_2^1]}{C_0}$$

$$f_{N_2} = \frac{[N_2]}{C_0}$$

Eqs. (1)–(11) were used to fit the population of states as a function of temperature for TF (f_U $f_{I_2^3}$ $f_{I_2^2}$ $f_{I_2^1}$ f_{N_2}). The fractional population of the different TF species during thermal unfolding is shown in Fig. 2. Simulated apparent heat capacity as a function of temperature for TF using this 5-state model is shown in Fig. 3A and the related thermodynamic parameters are shown in Table 1. As shown in Fig. 3A, the simulated apparent heat capacity produced by this 5-state model is still not a perfect fit to the experimental data, suggesting that the thermal unfolding of TF is even more complicated than the proposed mechanism. However, this is the best simulation that can be obtained from the thermogram profile of TF during thermal unfolding. For example, if we considered only two dimeric intermediates in the thermal unfolding process of TF, $N_2 \overset{K_1}{\leftrightarrow} I_2^1 \overset{K_2}{\leftrightarrow} I_2^2 \overset{K_D}{\leftrightarrow} 2U$, the simulated apparent heat capacity deviated dramatically from the experimental data (Fig. 3B).

According to this five-state thermal unfolding model, dimeric TF unfolds via three dimeric intermediates to reach the unfolded monomeric state. The relative abundance of the thermal species (N_2, I_2^1, I_2^2, I_2^3 and U) was determined as a function of the temperature. From Fig. 2, we can see that the population of the native dimer of TF decreases with increasing temperature and reaches 50% at around 315 K. The population of I_2^1 increases with decreasing N_2 and it is

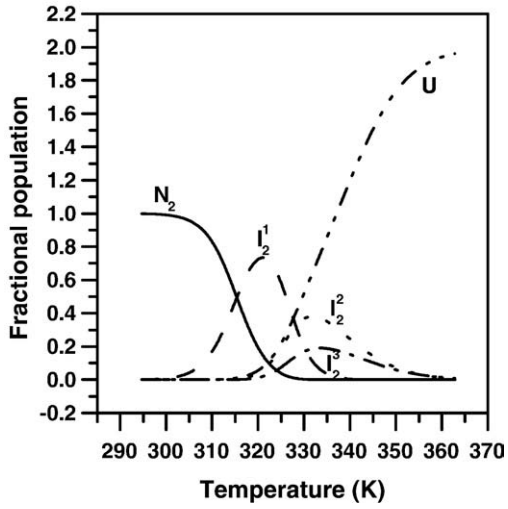

Fig. 2. Temperature-dependence of the fractional population of TF and the intermediates during thermal unfolding. Native dimeric TF, N_2, solid line; dimeric intermediate, I_2^1, dash line; dimeric intermediate, I_2^2, dot line; dimeric intermediate, I_2^3, dash dot line; unfold monomer, U, dash dot dot line.

Table 1
Thermodynamic parameters for the thermal unfolding of TF, MC and NM derived from simulation of DSC data

Protein (model)	Term	Tm (K)	ΔH (kcal mol^{-1})	ΔS (cal mol^{-1} K^{-1})
TF (5-state model)	K_1	315.4±0.5	57±6	182±20
	K_2	328.2±0.2	74±7	224±22
	K_3	357.3±0.2	7±1	19±2
	K_D	369.4±0.2	40±5	107±13
MC (4-state model)	K_1	315.2±0.3	3±0.5	10±1
	K_2	322.0±0.2	59±6	184±17
	K_D	365.8±0.4	35±4	96±10
MC (3-state model)	K_1	320.3±0.2	69±7	214±20
	K_D	369.0±0.3	29±3	79±8
NM (3-state model)	K_1	315.5±0.1	46±5	145±16
	K_D	318.7±0.3	41±5	129±14

Data for each protein corresponds to the mean±S.E. (standard error) of three independent experiments.

maximally populated at around 322 K; then the population of I_2^1 decreases accompanying the increase in population of I_2^2 and I_2^3. The appearance of U accompanies the appearance of I_2^2 and I_2^3 at around 320 K. When population of I_2^2 and I_2^3 reaches a maximum, population of both N_2 and I_2^1 is negligible. Finally, when the temperature is higher

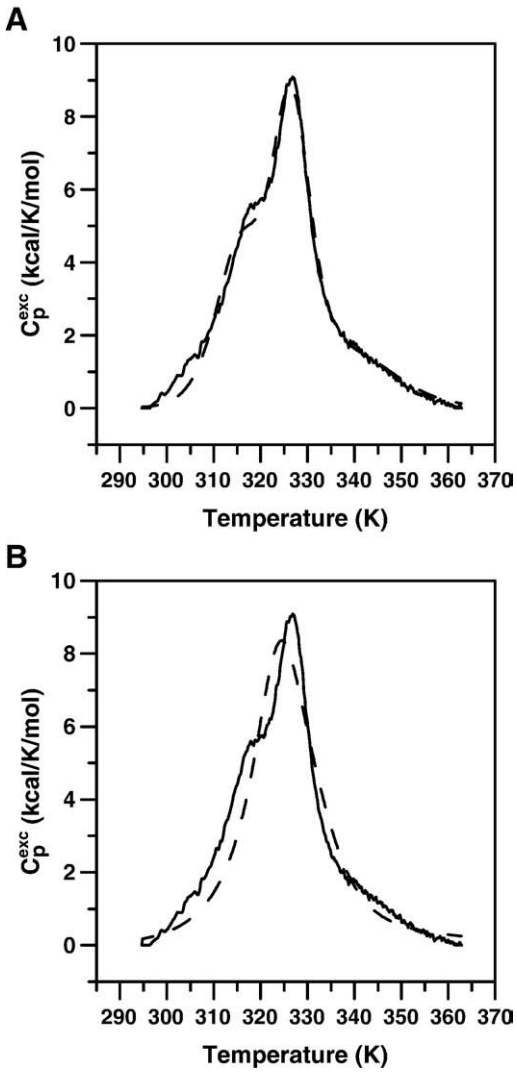

Fig. 3. Simulated apparent heat capacity as a function of temperature for TF using the 5-state model (A), and the 4-state model (B). The experimental data were shown as straight lines and the simulated apparent capacities were shown as dash lines.

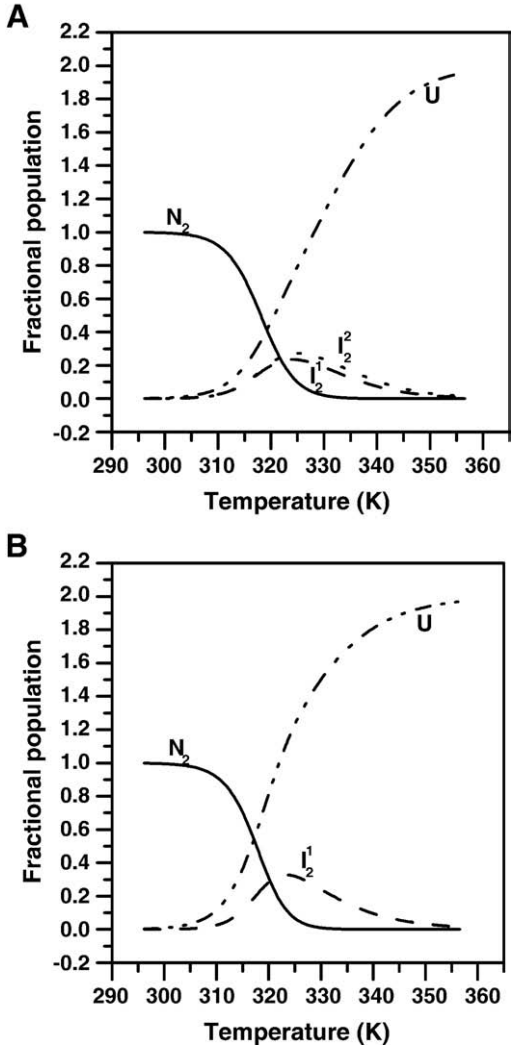

Fig. 4. Temperature-dependence of the fractional population of MC and the intermediates. The thermal unfolding of MC was analyzed by the 4-state model (A) and 3-state model (B), respectively. Native dimeric MC, N_2, solid line; dimeric intermediate I_2^1, dash line; dimeric intermediate I_2^2, dot line; unfold monomer U, dash dot dot line.

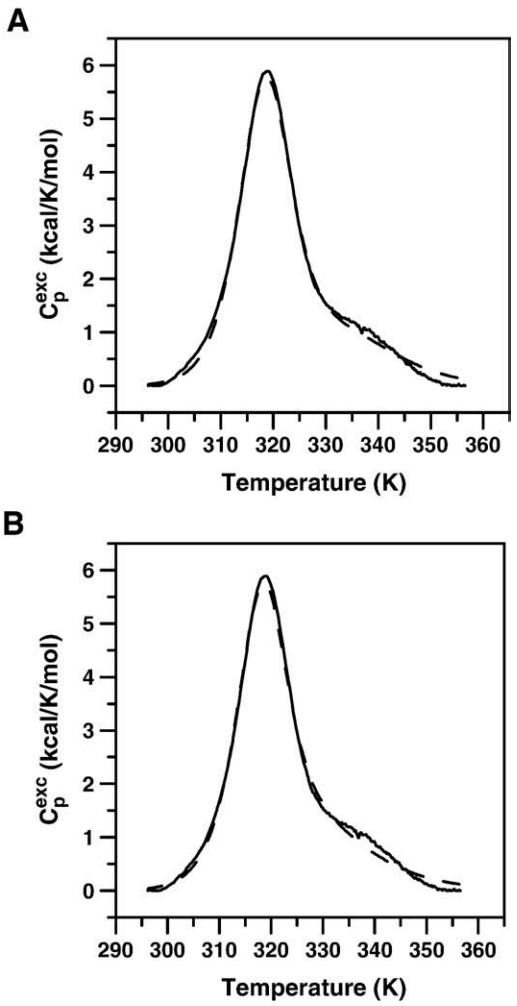

Fig. 5. Simulated apparent heat capacity as a function of temperature for MC using the 4-state model (A) and the 3-state model (B), respectively. The experimental data were shown as straight lines and the simulated apparent capacities were shown as dash lines.

than 360 K, all of the species are converted to unfolded monomer and so the concentration of unfolded monomer is two fold the initial concentration of the dimeric state. Thus, the relative fractional population of the unfolded monomer reaches 2.0. The presence of dimeric intermediates is well supported by DSS cross-linking experiments (see below), confirming the conclusion that the thermal unfolding of TF is a stepwise process via a number of thermostable dimeric intermediates. In our previous studies, a stable complex between folding intermediates of GAPDH (or BCA II) and dimeric TF was characterized and suggested that dimeric TF plays an important role in assisting protein folding *in vitro* [20,30]. Based on this, we speculate that the thermostable dimeric intermediates of TF may be populated when the cell is subjected to heat shock and so the dimeric species of TF could play some protective role *in vivo*.

3.3. Thermal unfolding of MC, in which the N domain of TF is truncated, involves population of a dimeric intermediate

Simulated data show that the thermal unfolding process of MC can be described well by models involving either one or two dimeric intermediates.

The more complex model implies three consecutive steps, including two dimeric intermediates:

$$N_2 \overset{K_1}{\longleftrightarrow} I_2^1 \overset{K_2}{\longleftrightarrow} I_2^2 \overset{K_D}{\longleftrightarrow} 2U$$

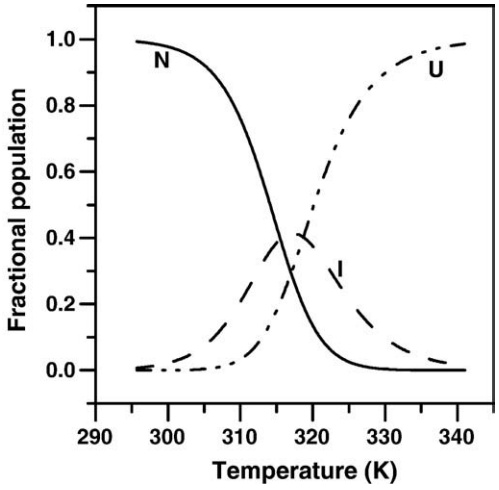

Fig. 6. Temperature-dependence of the fractional population of NM and the intermediates. Native monomeric NM, *N*, solid line; monomeric intermediate, *I*, dash line; unfolded monomer, *U*, dash dot dot line.

The simplest model implies two consecutive steps, including only one dimeric intermediate:

$$N_2 \overset{K_1}{\longleftrightarrow} I_2^1 \overset{K_D}{\longleftrightarrow} 2U$$

The processes were fitted using a similar method to that used for TF and the best fit of the data is shown in Figs. 4 and 5. The fractional population of the different species of MC populated during thermal unfolding is shown in Fig. 4A and B. The simulated apparent heat capacity as a function of temperature for MC using the 4-state or 3-state models is shown in Fig. 5A and B, and the related thermodynamic parameters are shown in Table 1. In fact, the two intermediates show only slight differences in the temperature dependence of their distribution, as shown in Fig. 4, and the correspondence between experimental and simulated apparent heat capacities is not improved by involving a second intermediate (Fig. 5A and B), suggesting that a single dimeric intermediate is sufficient to account for the observed results. The presence of a dimeric intermediate of MC was also confirmed by DSS cross-linking experiments (see below).

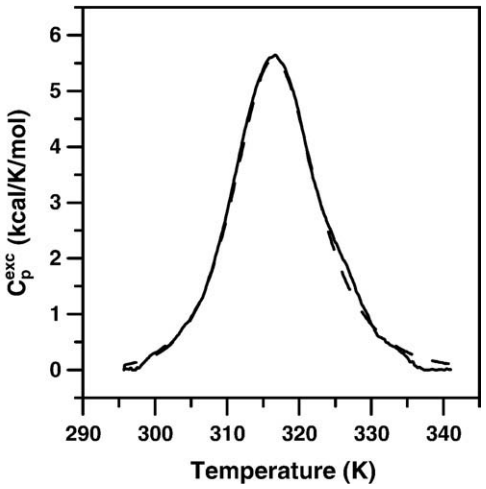

Fig. 7. Simulated apparent heat capacity as a function of temperature for NM using the 3-state model. The experimental data were shown as straight line and the simulated apparent capacities were shown as dash line.

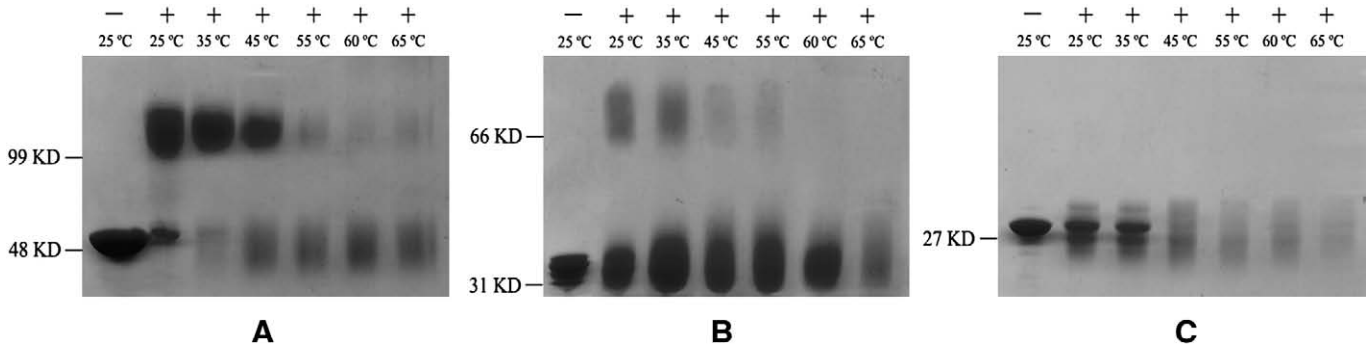

Fig. 8. Cross-linking of TF (A), MC (B) and NM (C) at different temperature. TF, MC and NM at 20 μM were cross-linked by 6 mM DSS at different temperature for 30 min. Products were separated by SDS-PAGE (8% acrylamide gel). The cross-linking temperatures, with (+) or without (−) DSS were shown at the top of each gel.

3.4. Thermal unfolding of NM, in which the C domain of TF is truncated, involves a single monomeric intermediate

Simulated data show that there is only one possible model to fit the thermal unfolding process of the NM fragment as shown below:

$$N \overset{K_1}{\longleftrightarrow} I \overset{K_D}{\longleftrightarrow} U$$

The fractional population of the different species of NM during thermal unfolding is shown in Fig. 6. The simulated apparent heat capacity as a function of temperature for NM is shown in Fig. 7, and the related thermodynamic parameters are shown in Table 1. It is interesting that the thermal unfolding of NM is distinctly different from that of TF and MC. NM is initially monomeric and unfolds via a monomeric intermediate to reach the unfolded state. That the NM fragment does not form a dimer under the experimental conditions used is also supported by DSS cross-linking experiments (see results below). This provides further evidence that the C-terminal domain is critical for dimerization of the TF molecule.

3.5. Dimeric forms of TF and its mutants identified by DSS cross-linking

To confirm that dimeric forms of TF and its mutants are populated during thermal unfolding, DSS cross-linking was performed at different temperatures. As shown in Fig. 8, a dimeric band was clearly apparent at 25 °C for TF and MC. However, no dimeric band was observed for NM, implying that only TF and MC, those proteins that contain the C domain, form a dimer under the experimental conditions used. This provides further evidence that the C-terminal domain of TF plays a vital role in forming and stabilizing the dimeric structure of the TF molecule. With increasing temperature, TF and MC could still be cross-linked by DSS, further confirming the presence of dimeric intermediates of TF and MC during thermal unfolding. The cross-linking patterns (Fig. 8) are consistent with the fractional distribution results (Figs. 2, 4 and 6) and so strongly support the thermal unfolding models of TF and its mutants derived from simulation of the DSC data.

4. Conclusion

The thermal unfolding of TF and its mutants measured by US-DSC is quite different from that observed by urea [18] or guanidine denaturation [20]. The population of multiple thermostable dimeric intermediates of TF during thermal unfolding was indicated by simulation of the DSC data and confirmed by DSS cross-linking experiments. By comparing the thermal unfolding of the intact TF molecule and the domain truncation mutants, NM and MC, we provide further evidence that the C-terminal domain of TF plays a vital role in forming and stabilizing the dimeric structure of the TF molecule.

In *E. coli* cells, the majority of ribosomes are predicted to exist in a 1:1 complex with TF [5,15] and TF is present in 2–3 fold molar excess over ribosomes, with the majority of free TF present as a dimer [31]. The dimeric intermediates of TF populated during thermal denaturation and identified by DSC in this investigation may be important under physiological conditions when the cell is subjected to heat shock. The thermally unfolded intermediates of TF may serve as a "binding chaperone" to maintain non-native protein in a refolding competent conformation and cooperate with downstream molecular chaperones to facilitate post-translational or post-stress protein folding [21].

Acknowledgements

The present study was supported in part by the Chinese Ministry of Science and Technology (G1999075608), the Chinese National Natural Science Foundation (30470363, 30620130109, 30670428), and a CAS Knowledge Innovation Grant (KSCX2-SW214-3). The authors would like to thank Dr. S. Perrett of this institute for her critical reading of this paper and helpful suggestions.

References

[1] T. Hesterkamp, S. Hauser, H. Lütcke, B. Bukau, *Escherichia coli* trigger factor is a prolyl isomerase that associates with nascent polypeptide chains, Proc. Natl. Acad. Sci. U.S.A. 93 (1996) 4437–4441.
[2] Q.A. Valent, D.A. Kendall, S. High, B. Oudega, J. Luirink, Early events in preprotein recognition in *E. coli*: interaction of SRP and trigger factor with nascent polypeptides, EMBO J. 14 (1995) 5494–5505.
[3] G. Stoller, K.P. Rücknagel, K.H. Nierhaus, F.X. Schmid, G. Fischer, J.U. Rahfeld, A ribosome-associated peptidyl–prolyl *cis*/*trans* isomerase identified as the trigger factor, EMBO J. 14 (1995) 4939–4948.
[4] C. Scholz, G. Stoller, G. Fischer, F.X. Schmid, Cooperation of enzymatic and chaperone functions of trigger factor in the catalysis of protein folding, EMBO J. 16 (1997) 54–58.
[5] G. Kramer, T. Rauch, W. Rist, S. Vorderwülbecke, H. Patzelt, A. Schulze-Specking, N. Ban, E. Deuerling, B. Bukau, L23 protein functions as a chaperone docking site on the ribosome, Nature 419 (2002) 171–174.
[6] G. Blaha, D.N. Wilson, G. Stoller, G. Fischer, R. Willumeit, K.H. Nierhaus, Localization of the trigger factor binding site on the ribosomal 50S subunit, J. Mol. Biol. 326 (2003) 887–897.
[7] G. Stoller, T. Tradler, K.P. Rücknagel, J.U. Rahfeld, G. Fischer, An 11.8 kDa proteolytic fragment of *E. coli* trigger factor represents the domain carrying the peptidyl–prolyl *cis*/*trans* isomerase activity, FEBS Lett. 384 (1996) 117–122.
[8] T. Zarnt, T. Tradler, G. Stoller, C. Scholz, F.X. Schmid, G. Fischer, Modular structure of the trigger factor required for high activity in protein folding, J. Mol. Biol. 271 (1997) 827–837.
[9] T. Hesterkamp, E. Deuerling, B. Bukau, The amino-terminal 118 amino acids of *Escherichia coli* trigger factor constitute a domain that is necessary and sufficient for binding to ribosomes, J. Biol. Chem. 272 (1997) 21865–21871.
[10] D. Baram, E. Pyetan, A. Sittner, T. Auerbach-Nevo, A. Bashan, A. Yonath, Structure of trigger factor binding domain in biologically homologous complex with eubacterial ribosome reveals its chaperone action, Proc. Natl. Acad. Sci. U.S.A. 102 (2005) 12017–12022.
[11] A. Hoffmann, F. Merz, A. Rutkowska, B. Zachmann-Brand, E. Deuerling, B. Bukau, Trigger factor forms a protective shield for nascent polypeptides at the ribosome, J. Biol. Chem. 281 (2006) 6539–6545.

[12] P. Genevaux, F. Keppel, F. Schwager, P.S. Langendijk-Genevaux, F.U. Hartl, C. Georgopoulos, In vivo analysis of the overlapping functions of DnaK and trigger factor, EMBO Rep. 5 (2004) 195–200.
[13] G. Kramer, A. Rutkowska, R. Wegrzyn, H. Patzelt, T.A. Kurz, F. Merz, T. Rauch, S. Vorderwülbecke, E. Deuerling, B. Bukau, Functional dissection of *Escherichia coli* trigger factor: unravelling the function of individual domains, J. Bacteriol. 186 (2004) 3777–3784.
[14] F. Merz, A. Hoffmann, A. Rutkowska, B. Zachmann-Brand, B. Bukau, E. Deuerling, The C-terminal domain of *Escherichia coli* trigger factor represents the central module of its chaperone activity, J. Biol. Chem. 281 (2006) 31963–31971.
[15] L. Ferbitz, H. Patzelt, B. Bukau, E. Deuerling, N. Ban, Trigger factor in complex with the ribosome forms a molecular cradle for nascent proteins, Nature 431 (2004) 590–596.
[16] R.L. Baldwin, G.D. Rose, Is protein folding hierarchic? II. Folding intermediates and transition states, Trends Biochem. Sci. 24 (1999) 77–83.
[17] M. Arai, K. Kuwajima, Role of the molten globule state in protein folding, Adv. Protein Chem. 53 (2000) 209–282.
[18] A.L. Fink, Compact intermediate states in protein folding, Annu. Rev. Biophys. Biomol. Struct. 24 (1995) 495–522.
[19] O.B. Ptitsyn, Molten globule and protein folding, Adv. Protein Chem. 47 (1995) 83–229.
[20] C.P. Liu, Z.Y. Li, G.C. Huang, S. Perrett, J.M. Zhou, Two distinct intermediates of trigger factor are populated during guanidine denaturation, Biochimie 87 (2005) 1023–1031.
[21] C.P. Liu, S. Perrett, J.M. Zhou, Dimeric trigger factor stably binds folding-competent intermediates and cooperates with the DnaK-DnaJ-GrpE chaperone system to allow refolding, J. Biol. Chem. 280 (2005) 13315–13320.
[22] E. Freire, R.L. Biltonen, Statistical mechanical deconvolution of thermal transitions in macromolecules. I. Theory and application to homogeneous systems, Biopolymers 17 (1978) 463–479.
[23] Y. Shi, D.J. Fan, S.X. Li, H.J. Zhang, S. Perrett, J.M. Zhou, Identification of a potential hydrophobic peptide binding site in the C-terminal arm of trigger factor, Protein Sci. 16 (2007) 1165–1175.
[24] L.L. Zeng, L. Yu, Z.Y. Li, S. Perrett, J.M. Zhou, Effect of C-terminal truncation on the molecular chaperone function and dimerization of *Escherichia coli* trigger factor, Biochimie 88 (2006) 613–619.
[25] S.C. Gill, P.H. von Hippel, Calculation of protein extinction coefficients from amino acid sequence data, Anal. Biochem. 182 (1989) 319–326.
[26] A.V. Ludlam, B.A. Moore, Z.H. Xu, The crystal structure of ribosomal chaperon trigger factor from vibrio cholerae, Proc. Natl. Acad. Sci. U.S.A. 101 (2004) 13436–13441.
[27] C.M. Kaiser, H.C. Chang, V.R. Agashe, S.K. Lakshmipathy, S.A. Etchells, M. Hartl, F.U. Hayer-Hartl, J.M. Barral, Real-time observation of trigger factor function on translating ribosomes, Nature 444 (2006) 455–460.
[28] R. Maier, B. Eckert, C. Scholz, H. Lilie, F.X. Schmid, Interaction of trigger factor with the ribosome, J. Mol. Biol. 326 (2003) 585–592.
[29] H. Patzelt, G. Kramer, T. Rauch, H.J. Schönfeld, B. Bukau, E. Deuerling, Three-state equilibrium of *Escherichia coli* trigger factor, Biol. Chem. 383 (2002) 1611–1619.
[30] C.P. Liu, J.M. Zhou, Trigger factor-assisted folding of bovine carbonic anhydrase II, Biochem. Biophys. Res. Commun. 313 (2004) 509–515.
[31] H. Patzelt, S. Rüdiger, D. Brehmer, G. Kramer, S. Vorderwülbecke, E. Schaffitzel, A. Waitz, T. Hesterkamp, L. Dong, J. Schneider-Mergener, B. Bukau, E. Deuerling, Binding specificity of *Escherichia coli* trigger factor, Proc. Natl. Acad. Sci. U.S.A. 98 (2001) 14244–14249.